Cold-nuclear-matter effects on heavy-quark production at forward and backward rapidity in d+Au collisions at $\sqrt{s_{_{NN}}} = 200$ GeV

A. Adare,[13] C. Aidala,[38,42,43] N.N. Ajitanand,[60] Y. Akiba,[55,56] R. Akimoto,[12] H. Al-Bataineh,[49] H. Al-Ta'ani,[49]
J. Alexander,[60] K.R. Andrews,[1] A. Angerami,[14] K. Aoki,[34,55] N. Apadula,[61] E. Appelt,[65] Y. Aramaki,[12,55]
R. Armendariz,[8] E.C. Aschenauer,[7] E.T. Atomssa,[35] R. Averbeck,[61] T.C. Awes,[51] B. Azmoun,[7] V. Babintsev,[24]
M. Bai,[6] G. Baksay,[19] L. Baksay,[19] B. Bannier,[61] K.N. Barish,[8] B. Bassalleck,[48] A.T. Basye,[1] S. Bathe,[5,8,56]
V. Baublis,[54] C. Baumann,[44] A. Bazilevsky,[7] S. Belikov,[7,*] R. Belmont,[65] J. Ben-Benjamin,[45] R. Bennett,[61]
J.H. Bhom,[69] D.S. Blau,[33] J.S. Bok,[69] K. Boyle,[56,61] M.L. Brooks,[38] D. Broxmeyer,[45] H. Buesching,[7]
V. Bumazhnov,[24] G. Bunce,[7,56] S. Butsyk,[38] S. Campbell,[61] A. Caringi,[45] P. Castera,[61] C.-H. Chen,[61] C.Y. Chi,[14]
M. Chiu,[7] I.J. Choi,[25,69] J.B. Choi,[10] R.K. Choudhury,[4] P. Christiansen,[40] T. Chujo,[64] P. Chung,[60] O. Chvala,[8]
V. Cianciolo,[51] Z. Citron,[61] B.A. Cole,[14] Z. Conesa del Valle,[35] M. Connors,[61] M. Csanád,[17] T. Csörgő,[68]
T. Dahms,[61] S. Dairaku,[34,55] I. Danchev,[65] K. Das,[20] A. Datta,[42] G. David,[7] M.K. Dayananda,[21] A. Denisov,[24]
A. Deshpande,[56,61] E.J. Desmond,[7] K.V. Dharmawardane,[49] O. Dietzsch,[58] A. Dion,[28,61] M. Donadelli,[58]
O. Drapier,[35] A. Drees,[61] K.A. Drees,[6] J.M. Durham,[38,61] A. Durum,[24] D. Dutta,[4] L. D'Orazio,[41] S. Edwards,[20]
Y.V. Efremenko,[51] F. Ellinghaus,[13] T. Engelmore,[14] A. Enokizono,[51] H. En'yo,[55,56] S. Esumi,[64] B. Fadem,[45]
D.E. Fields,[48] M. Finger,[9] M. Finger, Jr.,[9] F. Fleuret,[35] S.L. Fokin,[33] Z. Fraenkel,[67,*] J.E. Frantz,[50,61] A. Franz,[7]
A.D. Frawley,[20] K. Fujiwara,[55] Y. Fukao,[55] T. Fusayasu,[47] C. Gal,[61] I. Garishvili,[62] A. Glenn,[37] H. Gong,[61]
X. Gong,[60] M. Gonin,[35] Y. Goto,[55,56] R. Granier de Cassagnac,[35] N. Grau,[2,14] S.V. Greene,[65] G. Grim,[38]
M. Grosse Perdekamp,[25] T. Gunji,[12] L. Guo,[38] H.-Å. Gustafsson,[40,*] J.S. Haggerty,[7] K.I. Hahn,[18] H. Hamagaki,[12]
J. Hamblen,[62] R. Han,[53] J. Hanks,[14] C. Harper,[45] K. Hashimoto,[55,57] E. Haslum,[40] R. Hayano,[12] X. He,[21]
M. Heffner,[37] T.K. Hemmick,[61] T. Hester,[8] J.C. Hill,[28] M. Hohlmann,[19] R.S. Hollis,[8] W. Holzmann,[14] K. Homma,[23]
B. Hong,[32] T. Horaguchi,[23,64] Y. Hori,[12] D. Hornback,[51,62] S. Huang,[65] T. Ichihara,[55,56] R. Ichimiya,[55]
H. Iinuma,[31] Y. Ikeda,[64] K. Imai,[29,34,55] M. Inaba,[64] A. Iordanova,[8] D. Isenhower,[1] M. Ishihara,[55] M. Issah,[65]
D. Ivanischev,[54] Y. Iwanaga,[23] B.V. Jacak,[61] J. Jia,[7,60] X. Jiang,[38] J. Jin,[14] D. John,[62] B.M. Johnson,[7]
T. Jones,[1] K.S. Joo,[46] D. Jouan,[52] D.S. Jumper,[1] F. Kajihara,[12] J. Kamin,[61] S. Kaneti,[61] B.H. Kang,[22]
J.H. Kang,[69] J.S. Kang,[22] J. Kapustinsky,[38] K. Karatsu,[34,55] M. Kasai,[55,57] D. Kawall,[42,56] M. Kawashima,[55,57]
A.V. Kazantsev,[33] T. Kempel,[28] A. Khanzadeev,[54] K.M. Kijima,[23] J. Kikuchi,[66] A. Kim,[18] B.I. Kim,[32] D.J. Kim,[30]
E.-J. Kim,[10] Y.-J. Kim,[25] Y.K. Kim,[22] E. Kinney,[13] Á. Kiss,[17] E. Kistenev,[7] D. Kleinjan,[8] P. Kline,[61]
L. Kochenda,[54] B. Komkov,[54] M. Konno,[64] J. Koster,[25] D. Kotov,[54] A. Král,[15] A. Kravitz,[14] G.J. Kunde,[38]
K. Kurita,[55,57] M. Kurosawa,[55] Y. Kwon,[69] G.S. Kyle,[49] R. Lacey,[60] Y.S. Lai,[14] J.G. Lajoie,[28] A. Lebedev,[28]
D.M. Lee,[38] J. Lee,[18] K.B. Lee,[32] K.S. Lee,[32] S.H. Lee,[61] S.R. Lee,[10] M.J. Leitch,[38] M.A.L. Leite,[58] X. Li,[11]
P. Lichtenwalner,[45] P. Liebing,[56] S.H. Lim,[69] L.A. Linden Levy,[13] T. Liška,[15] H. Liu,[38] M.X. Liu,[38] B. Love,[65]
D. Lynch,[7] C.F. Maguire,[65] Y.I. Makdisi,[6] M.D. Malik,[48] A. Manion,[61] V.I. Manko,[33] E. Mannel,[14] Y. Mao,[53,55]
H. Masui,[64] F. Matathias,[14] M. McCumber,[13,61] P.L. McGaughey,[38] D. McGlinchey,[13,20] C. McKinney,[25]
N. Means,[61] M. Mendoza,[8] B. Meredith,[25] Y. Miake,[64] T. Mibe,[31] A.C. Mignerey,[41] K. Miki,[55,64] A. Milov,[7,67]
J.T. Mitchell,[7] Y. Miyachi,[55,63] A.K. Mohanty,[4] H.J. Moon,[46] Y. Morino,[12] A. Morreale,[8] D.P. Morrison,[7,†]
S. Motschwiller,[45] T.V. Moukhanova,[33] T. Murakami,[34] J. Murata,[55,57] S. Nagamiya,[31] J.L. Nagle,[13,‡] M. Naglis,[67]
M.I. Nagy,[68] I. Nakagawa,[55,56] Y. Nakamiya,[23] K.R. Nakamura,[34,55] T. Nakamura,[55] K. Nakano,[55] S. Nam,[18]
J. Newby,[37] M. Nguyen,[61] M. Nihashi,[23] R. Nouicer,[7] A.S. Nyanin,[33] C. Oakley,[21] E. O'Brien,[7] S.X. Oda,[12]
C.A. Ogilvie,[28] M. Oka,[64] K. Okada,[56] Y. Onuki,[55] A. Oskarsson,[40] M. Ouchida,[23,55] K. Ozawa,[12] R. Pak,[7]
V. Pantuev,[26,61] V. Papavassiliou,[49] B.H. Park,[22] I.H. Park,[18] S.K. Park,[32] W.J. Park,[32] S.F. Pate,[49] L. Patel,[21]
H. Pei,[28] J.-C. Peng,[25] H. Pereira,[16] D.Yu. Peressounko,[33] R. Petti,[61] C. Pinkenburg,[7] R.P. Pisani,[7] M. Proissl,[61]
M.L. Purschke,[7] H. Qu,[21] J. Rak,[30] I. Ravinovich,[67] K.F. Read,[51,62] S. Rembeczki,[19] K. Reygers,[44] V. Riabov,[54]
Y. Riabov,[54] E. Richardson,[41] D. Roach,[65] G. Roche,[39] S.D. Rolnick,[8] M. Rosati,[28] C.A. Rosen,[13]
S.S.E. Rosendahl,[40] P. Ružička,[27] B. Sahlmueller,[44,61] N. Saito,[31] T. Sakaguchi,[7] K. Sakashita,[55,63] V. Samsonov,[54]
S. Sano,[12,66] M. Sarsour,[21] T. Sato,[64] M. Savastio,[61] S. Sawada,[31] K. Sedgwick,[8] J. Seele,[13] R. Seidl,[25,56] R. Seto,[8]
D. Sharma,[67] I. Shein,[24] T.-A. Shibata,[55,63] K. Shigaki,[23] H.H. Shim,[32] M. Shimomura,[64] K. Shoji,[34,55] P. Shukla,[4]
A. Sickles,[7] C.L. Silva,[28] D. Silvermyr,[51] C. Silvestre,[16] K.S. Sim,[32] B.K. Singh,[3] C.P. Singh,[3] V. Singh,[3]
M. Slunečka,[9] T. Sodre,[45] R.A. Soltz,[37] W.E. Sondheim,[38] S.P. Sorensen,[62] I.V. Sourikova,[7] P.W. Stankus,[51]
E. Stenlund,[40] S.P. Stoll,[7] T. Sugitate,[23] A. Sukhanov,[7] J. Sun,[61] J. Sziklai,[68] E.M. Takagui,[58] A. Takahara,[12]

A. Taketani,[55,56] R. Tanabe,[64] Y. Tanaka,[47] S. Taneja,[61] K. Tanida,[34,55,56,59] M.J. Tannenbaum,[7] S. Tarafdar,[3] A. Taranenko,[60] E. Tennant,[49] H. Themann,[61] D. Thomas,[1] T.L. Thomas,[48] M. Togawa,[56] A. Toia,[61] L. Tomášek,[27] M. Tomášek,[27] H. Torii,[23] R.S. Towell,[1] I. Tserruya,[67] Y. Tsuchimoto,[23] K. Utsunomiya,[12] C. Vale,[7] H. Valle,[65] H.W. van Hecke,[38] E. Vazquez-Zambrano,[14] A. Veicht,[14,25] J. Velkovska,[65] R. Vértesi,[68] M. Virius,[15] A. Vossen,[25] V. Vrba,[27] E. Vznuzdaev,[54] X.R. Wang,[49] D. Watanabe,[23] K. Watanabe,[64] Y. Watanabe,[55,56] Y.S. Watanabe,[12] F. Wei,[28] R. Wei,[60] J. Wessels,[44] S.N. White,[7] D. Winter,[14] C.L. Woody,[7] R.M. Wright,[1] M. Wysocki,[13] Y.L. Yamaguchi,[12,55] K. Yamaura,[23] R. Yang,[25] A. Yanovich,[24] J. Ying,[21] S. Yokkaichi,[55,56] J.S. Yoo,[18] Z. You,[38,53] G.R. Young,[51] I. Younus,[36,48] I.E. Yushmanov,[33] W.A. Zajc,[14] A. Zelenski,[6] and S. Zhou[11]

(PHENIX Collaboration)

[1]*Abilene Christian University, Abilene, Texas 79699, USA*
[2]*Department of Physics, Augustana College, Sioux Falls, South Dakota 57197, USA*
[3]*Department of Physics, Banaras Hindu University, Varanasi 221005, India*
[4]*Bhabha Atomic Research Centre, Bombay 400 085, India*
[5]*Baruch College, City University of New York, New York, New York, 10010 USA*
[6]*Collider-Accelerator Department, Brookhaven National Laboratory, Upton, New York 11973-5000, USA*
[7]*Physics Department, Brookhaven National Laboratory, Upton, New York 11973-5000, USA*
[8]*University of California - Riverside, Riverside, California 92521, USA*
[9]*Charles University, Ovocný trh 5, Praha 1, 116 36, Prague, Czech Republic*
[10]*Chonbuk National University, Jeonju, 561-756, Korea*
[11]*Science and Technology on Nuclear Data Laboratory, China Institute of Atomic Energy, Beijing 102413, P. R. China*
[12]*Center for Nuclear Study, Graduate School of Science, University of Tokyo, 7-3-1 Hongo, Bunkyo, Tokyo 113-0033, Japan*
[13]*University of Colorado, Boulder, Colorado 80309, USA*
[14]*Columbia University, New York, New York 10027 and Nevis Laboratories, Irvington, New York 10533, USA*
[15]*Czech Technical University, Zikova 4, 166 36 Prague 6, Czech Republic*
[16]*Dapnia, CEA Saclay, F-91191, Gif-sur-Yvette, France*
[17]*ELTE, Eötvös Loránd University, H - 1117 Budapest, Pázmány P. s. 1/A, Hungary*
[18]*Ewha Womans University, Seoul 120-750, Korea*
[19]*Florida Institute of Technology, Melbourne, Florida 32901, USA*
[20]*Florida State University, Tallahassee, Florida 32306, USA*
[21]*Georgia State University, Atlanta, Georgia 30303, USA*
[22]*Hanyang University, Seoul 133-792, Korea*
[23]*Hiroshima University, Kagamiyama, Higashi-Hiroshima 739-8526, Japan*
[24]*IHEP Protvino, State Research Center of Russian Federation, Institute for High Energy Physics, Protvino, 142281, Russia*
[25]*University of Illinois at Urbana-Champaign, Urbana, Illinois 61801, USA*
[26]*Institute for Nuclear Research of the Russian Academy of Sciences, prospekt 60-letiya Oktyabrya 7a, Moscow 117312, Russia*
[27]*Institute of Physics, Academy of Sciences of the Czech Republic, Na Slovance 2, 182 21 Prague 8, Czech Republic*
[28]*Iowa State University, Ames, Iowa 50011, USA*
[29]*Advanced Science Research Center, Japan Atomic Energy Agency, 2-4*
Shirakata Shirane, Tokai-mura, Naka-gun, Ibaraki-ken 319-1195, Japan
[30]*Helsinki Institute of Physics and University of Jyväskylä, P.O.Box 35, FI-40014 Jyväskylä, Finland*
[31]*KEK, High Energy Accelerator Research Organization, Tsukuba, Ibaraki 305-0801, Japan*
[32]*Korea University, Seoul, 136-701, Korea*
[33]*Russian Research Center "Kurchatov Institute", Moscow, 123098 Russia*
[34]*Kyoto University, Kyoto 606-8502, Japan*
[35]*Laboratoire Leprince-Ringuet, Ecole Polytechnique, CNRS-IN2P3, Route de Saclay, F-91128, Palaiseau, France*
[36]*Physics Department, Lahore University of Management Sciences, Lahore, Pakistan*
[37]*Lawrence Livermore National Laboratory, Livermore, California 94550, USA*
[38]*Los Alamos National Laboratory, Los Alamos, New Mexico 87545, USA*
[39]*LPC, Université Blaise Pascal, CNRS-IN2P3, Clermont-Fd, 63177 Aubiere Cedex, France*
[40]*Department of Physics, Lund University, Box 118, SE-221 00 Lund, Sweden*
[41]*University of Maryland, College Park, Maryland 20742, USA*
[42]*Department of Physics, University of Massachusetts, Amherst, Massachusetts 01003-9337, USA*
[43]*Department of Physics, University of Michigan, Ann Arbor, Michigan 48109-1040, USA*
[44]*Institut fur Kernphysik, University of Muenster, D-48149 Muenster, Germany*
[45]*Muhlenberg College, Allentown, Pennsylvania 18104-5586, USA*
[46]*Myongji University, Yongin, Kyonggido 449-728, Korea*
[47]*Nagasaki Institute of Applied Science, Nagasaki-shi, Nagasaki 851-0193, Japan*
[48]*University of New Mexico, Albuquerque, New Mexico 87131, USA*
[49]*New Mexico State University, Las Cruces, New Mexico 88003, USA*
[50]*Department of Physics and Astronomy, Ohio University, Athens, Ohio 45701, USA*
[51]*Oak Ridge National Laboratory, Oak Ridge, Tennessee 37831, USA*

[52]*IPN-Orsay, Universite Paris Sud, CNRS-IN2P3, BP1, F-91406, Orsay, France*
[53]*Peking University, Beijing 100871, P. R. China*
[54]*PNPI, Petersburg Nuclear Physics Institute, Gatchina, Leningrad region, 188300, Russia*
[55]*RIKEN Nishina Center for Accelerator-Based Science, Wako, Saitama 351-0198, Japan*
[56]*RIKEN BNL Research Center, Brookhaven National Laboratory, Upton, New York 11973-5000, USA*
[57]*Physics Department, Rikkyo University, 3-34-1 Nishi-Ikebukuro, Toshima, Tokyo 171-8501, Japan*
[58]*Universidade de São Paulo, Instituto de Física, Caixa Postal 66318, São Paulo CEP05315-970, Brazil*
[59]*Seoul National University, Seoul, Korea*
[60]*Chemistry Department, Stony Brook University, SUNY, Stony Brook, New York 11794-3400, USA*
[61]*Department of Physics and Astronomy, Stony Brook University, SUNY, Stony Brook, New York 11794-3400, USA*
[62]*University of Tennessee, Knoxville, Tennessee 37996, USA*
[63]*Department of Physics, Tokyo Institute of Technology, Oh-okayama, Meguro, Tokyo 152-8551, Japan*
[64]*Institute of Physics, University of Tsukuba, Tsukuba, Ibaraki 305, Japan*
[65]*Vanderbilt University, Nashville, Tennessee 37235, USA*
[66]*Waseda University, Advanced Research Institute for Science and*
Engineering, 17 Kikui-cho, Shinjuku-ku, Tokyo 162-0044, Japan
[67]*Weizmann Institute, Rehovot 76100, Israel*
[68]*Institute for Particle and Nuclear Physics, Wigner Research Centre for Physics, Hungarian*
Academy of Sciences (Wigner RCP, RMKI) H-1525 Budapest 114, POBox 49, Budapest, Hungary
[69]*Yonsei University, IPAP, Seoul 120-749, Korea*

(Dated: December 23, 2019)

The PHENIX experiment has measured open heavy-flavor production via semileptonic decay over the transverse momentum range $1 < p_T < 6$ GeV/c at forward and backward rapidity ($1.4 < |y| < 2.0$) in d+Au and p+p collisions at $\sqrt{s_{_{NN}}} = 200$ GeV. In central d+Au collisions an enhancement of heavy-flavor muon production is observed at backward rapidity, whereas suppression is seen at forward rapidity relative to the yield in p+p collisions scaled by the number of binary collisions. The difference observed between forward and backward rapidity exceeds predictions based on a model of initial parton density modification. These results can be used to probe predicted cold nuclear matter effects, which may significantly affect heavy-quark production at the Relativistic Heavy Ion Collider and the Large Hadron Collider, in addition to helping constrain the magnitude of charmonia breakup effects in nuclear matter.

PACS numbers: 25.75.Dw

Heavy quarks are essential probes of the evolution of the medium created in heavy-ion collisions, because they are produced in the early stages of nuclear collisions. Heavy-quark production has been measured via semileptonic decay electrons and muons, as well as fully reconstructed D mesons, at RHIC and the LHC [1, 2]. In p+p collisions, heavy-quark production tests perturbative quantum chromodynamics and provides a baseline for heavy-ion collisions [3–5]. In central Au+Au collisions at $\sqrt{s_{_{NN}}} = 200$ GeV, strong suppression of high transverse momentum (p_T) electrons from semileptonic decay of open heavy-flavor hadrons has been observed at midrapidity [6, 7]. At forward rapidity, a similar level of suppression has been measured for the production of heavy-flavor muons in central Cu+Cu collisions [8]. Although suppression of high p_T particles was predicted as an effect of partonic energy loss in the dense medium created in heavy-ion collisions [9–11], it is difficult to account for this comparable suppression solely with hot nuclear matter effects [8, 12]. To interpret such measurements, it is essential to probe underlying cold-nuclear-matter (CNM) effects, which may also be present.

Control experiments with d+Au collisions allow us to probe those CNM effects, including modifications of the parton distribution function (PDF) and k_T broadening, with minimal impact from the hot nuclear medium. Because heavy quarks are produced primarily by gluon fusion at RHIC, modification of the gluon density in the nucleus can be observed in the charm and bottom production rates [13, 14]. Based on PYTHIA [15] calculations, the average parton momentum fraction x in the Au nucleus leading to heavy-flavor muons with $1 < p_T^{\mu} < 6$ GeV/c at backward ($-2.0 < y < -1.4$, Au-going direction) and forward ($1.4 < y < 2.0$, d-going direction) rapidity is $\approx 8\times10^{-2}$ and $\approx 5\times10^{-3}$ for the antishadowing and shadowing regions, respectively. Parton energy loss and multiple scattering in the nucleus can change the resulting heavy-flavor hadron momentum spectrum [16]. Previous results in d+Au collisions at midrapidity show a significant enhancement of heavy-flavor electrons at moderate p_T [17]. In this Letter, we present measurements of the p_T spectra and the nuclear modification factor (R_{dA}) of negatively charged muons from open heavy flavor at forward and backward rapidity in d+Au collisions at $\sqrt{s_{_{NN}}} = 200$ GeV.

The d+Au and p+p data presented here were recorded with the PHENIX detector during the 2008 and 2009 RHIC running periods, respectively. The minimum-bias collision is selected by using the beam-beam counter (BBC) [18], and this selection covers $88 \pm 4\%$ ($55 \pm 5\%$)

of the total d+Au (p+p) inelastic cross section [19]. The integrated luminosity, sampled using single muon triggers [8] in coincidence with the minimum-bias trigger, used for this analysis of d+Au (p+p) collisions is 50 nb^{-1} (10 pb^{-1}). The d+Au collisions are categorized into five centrality classes: 0%–20%, 20%–40%, 40%–60%, 60%–88%, and 0%-100%, where 0%–20% represents the 20% highest multiplicity events, as determined by the amount of total charge deposited in the BBC on the Au-going side. For each centrality class, the average number of binary nucleon-nucleon collisions $\langle N_{\rm coll}\rangle$ is calculated from the BBC charge in a Glauber model [20]. Correction for the underlying event correlation and the efficiency of the BBC trigger to 100% is applied as in [21, 22]. The values of $\langle N_{\rm coll}\rangle$ for the five d+Au centrality classes specified above are 15.1 ± 1.0, 10.2 ± 0.7, 6.6 ± 0.4, 3.2 ± 0.2, and 7.6 ± 0.4 respectively.

Two muon spectrometers [23] provide full azimuthal coverage in the pseudorapidity range $-2.2 < \eta < -1.2$ (backward rapidity) and $1.2 < \eta < 2.4$ (forward rapidity). Each muon arm, located behind copper (19 cm) and iron (60 cm) absorbers, is composed of a muon tracker (MuTr) followed by a muon identifier (MuID). The MuTr comprises three stations of cathode strip chambers surrounded by a radial magnetic field, and the MuID comprises five interleaved layers of steel absorber and Iarocci tube planes. The MuTr provides the momentum measurement for charged tracks in the magnetic field. The momentum information for each charged track is then combined with its penetration depth reported by the MuID to provide effective discrimination between muons and hadrons (pion rejection rate: $\sim 10^{-3}$) [24].

Despite the large hadron rejection power of the muon arms and strict selection criteria, most of the tracks reaching the last MuID layer are not heavy-flavor muons. For $p_T < 3$ GeV/c the majority of these background tracks originate from the decays of light-flavor mesons (mostly $\pi^{\pm}$ and $K^{\pm}$) into muons before reaching the absorber material. Another source of background, called "punch-through hadrons," are the hadrons produced at the collision vertex, which penetrate all MuID layers. These become the dominant background at $p_T >$ 3 GeV/c. Other, less significant sources of background include muons from hadrons that decay inside the MuTr which are misreconstructed with erroneously high p_T, muons from heavy-flavor resonances (χ_c, J/ψ, ψ', and Υ), and muons from light vector mesons (ρ, ϕ, and ω). The backgrounds are subtracted as follows.

For each data set, we measure the double differential heavy-flavor muon invariant yield, defined as

$$\frac{d^2N^{\mu}}{2\pi p_T dp_T dy} = \frac{1}{2\pi p_T \Delta p_T \Delta y}\frac{N_I - N_C - N_F - N_{J/\psi}}{(N_{\rm evt}/c)A\epsilon} \tag{1}$$

where Δp_T and Δy are the bin widths in p_T and y; N_I is the number of inclusive muon candidates; N_C is the number of decay and punch-through hadron background tracks determined using a hadron cocktail method (described below); N_F is the estimated number of fake tracks that pass the selection criteria; $N_{J/\psi}$ is the number of muons from J/ψ decays; $N_{\rm evt}$ is the number of sampled events; $A\epsilon$ is the detector acceptance and efficiency correction; and c is the BBC bias correction factor for the trigger efficiency and centrality determination of events containing a heavy-flavor muon. The contribution from remaining background sources is less than 5% [8, 25]. Only negative muons are used, because the signal-to-background ratio is better than for positive muons [8]. The typical signal-to-background ratio, $N^{\mu}/(N_C + N_F + N_{J/\psi})$, increases from 0.3 at $p_T = 1$ GeV/c to 0.6 at $p_T = 6$ GeV/c. The hadron cocktail method estimates the overall background owing to light hadron sources using a fully data-driven GEANT simulation based on measured p_T spectra. Details on background estimation procedure and associated systematic uncertainty are described in [3, 8, 25].

Figure 1 shows the invariant yield of heavy-flavor muons in d+Au collisions at backward and forward rapidity along with the invariant yield in p+p collisions. The vertical bars represent statistical uncertainties, while boxes are systematic uncertainties in the acceptance and efficiency correction, background estimate, and trigger bias correction for each centrality class. The main source of the systematic uncertainties is the background estimate including initial hadron production ($\sim$10%) and hadron simulation ($\sim$10%). All components of the systematic uncertainty are added in quadrature. Solid lines show a modified Kaplan function $A\left[1 + (p_T/8.3\ ({\rm GeV}/c))^2\right]^{-3.9}$ [26], fit to the p_T spectrum in p+p collisions, and then scaled by $\langle N_{\rm coll}\rangle$ for each d+Au centrality class. The p+p results are consistent with previous PHENIX measurements [8].

To quantify nuclear effects in d+Au collisions, we calculate the ratio of heavy-flavor muon yields in d+Au to p+p collisions scaled by the average number of binary collisions for a given centrality bin,

$$R_{dA} = \frac{dN^{\mu^-}_{dA}/dp_T}{\langle N_{\rm coll}\rangle \times dN^{\mu^-}_{pp}/dp_T}. \tag{2}$$

Figure 2 shows R_{dA} as a function of p_T for heavy-flavor muons in different d+Au centrality classes. Vertical bars represent the statistical uncertainties for R_{dA}, which are the quadratic sum of the statistical uncertainties for the invariant yields of p+p and d+Au collisions. Boxes around the data points are the systematic uncertainties. The global scaling uncertainty in $\langle N_{\rm coll}\rangle$ and the BBC efficiency is shown as a box centered around unity at the right edge of the plot.

For the most peripheral collisions in both rapidity ranges, R_{dA} shows no overall modification. For the most central collisions, a clear enhancement is observed at

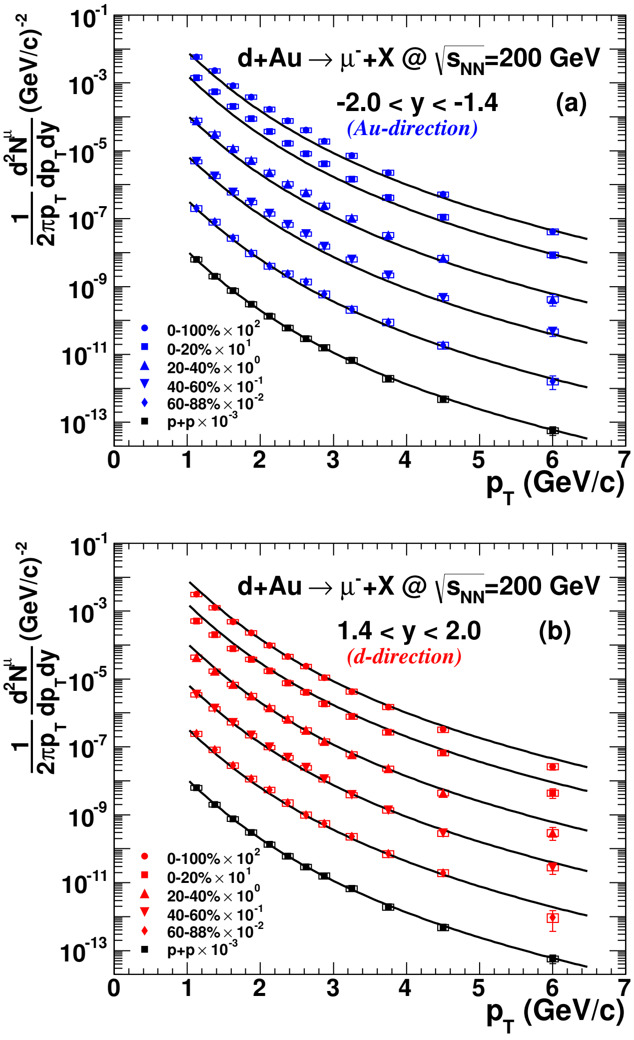

FIG. 1: (color online). Invariant yield of negatively charged heavy-flavor muons as a function of p_T in p+p collisions at $\sqrt{s_{NN}} = 200$ GeV (black squares) and in d+Au collisions for different centralities at (a) backward rapidity (Au-going) and (b) forward rapidity (d-going). The solid lines represent a fit to the p+p invariant yield, scaled by the number of binary collisions, $\langle N_{\rm coll}\rangle$, for each centrality class.

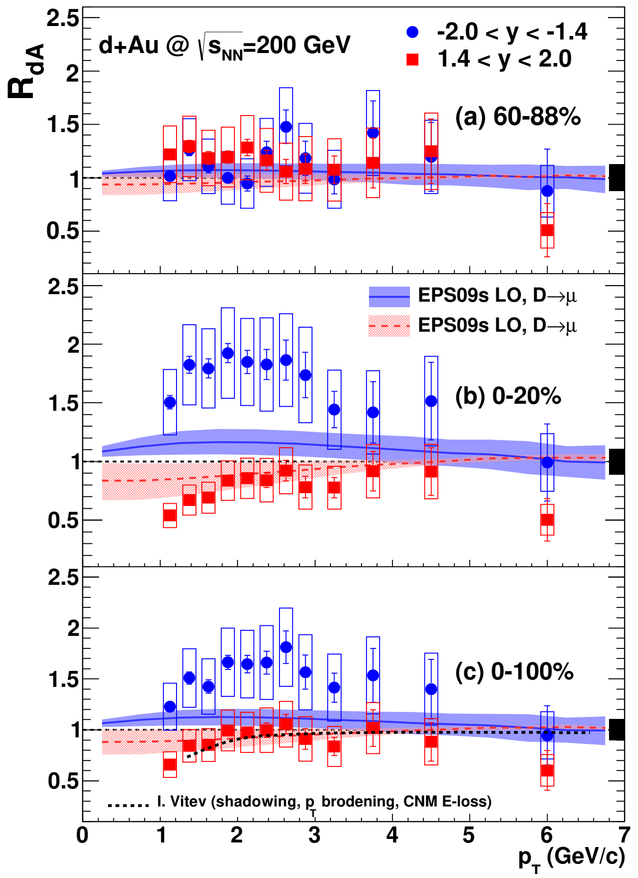

FIG. 2: (color online). The nuclear modification factor R_{dA}, for negatively charged heavy-flavor muons in d+Au collisions for the (a) 60%–88%, (b) 0%–20%, and (c) 0%–100% most central collisions. The black boxes on the right side indicate the global scaling uncertainty. The red dashed (blue solid) lines in each panel are calculations at forward (backward) rapidity based on the EPS09s nPDF set [14]. The theoretical calculation shown in (c) is for forward rapidity [16].

backward rapidity. This enhancement shows a p_T dependence consistent with p_T broadening and gluon antishadowing. A suppression is observed at forward rapidity in the most central collisions. At forward rapidity, p_T broadening is indicated by the slope of R_{dA}, combined with a suppression that could be caused by gluon shadowing and/or partonic energy loss in CNM.

The dotted line in Fig. 2(c) is a prediction of R_{dA} for muons from D and B mesons at forward rapidity, $y = 1.7$ [16, 27]. This prediction, including CNM effects such as shadowing, initial-state energy loss, and k_T broadening, is consistent with the data at forward rapidity for the 0%–100% centrality class. The same model, with additional energy loss in deconfined hot nuclear matter, also describes the forward heavy-flavor muon results in central Cu+Cu collisions within uncertainties [8]. This agreement and the suppression at forward rapidity in central d+Au collisions suggest that CNM effects may be important for the interpretation of the suppression of heavy-flavor muon production at forward rapidity at RHIC [8] and the Large Hadron Collider [28].

We use the EPS09s leading-order (LO) nuclear PDF (nPDF) set [14] to calculate R_{dA} for muons from D mesons at backward (solid lines) and forward (dashed lines) rapidity as described in [29]. The EPS09s nPDF further incorporates a spatial dependence within the nucleus to the nPDF. The modification of nPDF is determined based on the input parameters x, momentum transfer (Q^2) of charm production generated by PYTHIA [15], and transverse radial positions of binary collisions in the nucleus for each centrality class. The un-

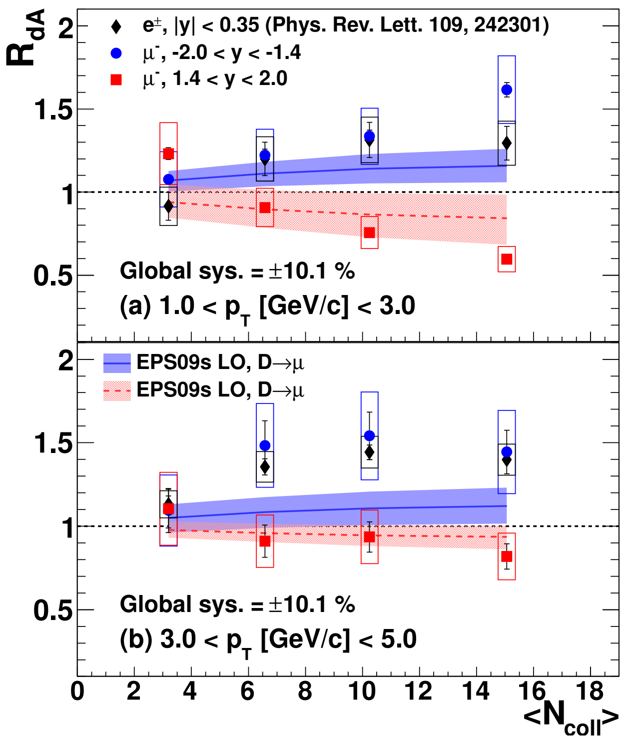

FIG. 3: (color online). Comparison of R_{dA} as a function of $\langle N_{\rm coll}\rangle$ for heavy-flavor leptons from different rapidity and p_T bins. Data in the top (bottom) panel are from low ($1 < p_T$ [GeV/c] < 3) and moderate ($3 < p_T$ [GeV/c] < 5) p_T ranges. Diamonds represent heavy-flavor electrons at midrapidity [17] and squares (circles) represent heavy-flavor muons at forward (backward) rapidity.

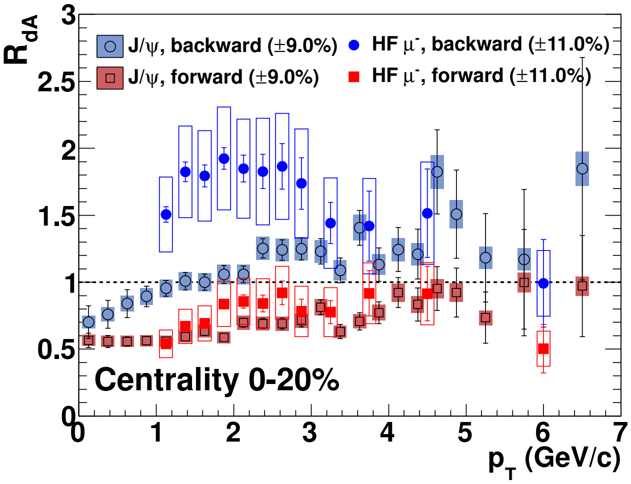

FIG. 4: (color online). The nuclear modification factor R_{dA} for J/ψ [21] and heavy-flavor muons for the 0%–20% centrality class. The global systematic uncertainty on each distribution is shown as a percentage in the legend.

certainty bands are calculated as described in [13]. From this calculation, we can take solely the initial parton density modification into account. In central collisions, shown in Fig. 2(b), the EPS09s nPDF based calculation does not reproduce the data at backward rapidity, particularly in the moderate p_T region; the difference is $\sim 2\sigma$ near $p_T = 2$ GeV/c. At forward rapidity, R_{dA} calculated with the EPS09s nPDF is consistent with the data over the entire p_T range within the systematic uncertainties of the data and calculation. The presence of other CNM effects is suggested, because the difference between forward and backward rapidity is significantly larger in the data than in the EPS09 nPDF calculation.

Figure 3 shows the heavy-flavor muon R_{dA} as a function of $\langle N_{\rm coll}\rangle$ for (a) $1.0 < p_T$ [GeV/c] < 3.0 and (b) $3.0 < p_T$ [GeV/c] < 5.0, compared to the heavy-flavor electron measurement at midrapidity [17]. Bars (boxes) around the data points represent the statistical (systematic) uncertainties determined as the quadratic sum of statistical (systematic) uncertainties on R_{dA} for each centrality class. In both p_T ranges midrapidity and backward rapidity results agree within systematic uncertainties, showing a large enhancement for more central collisions. At forward rapidity the low-p_T bin shows suppression increasing with centrality, whereas the high-p_T bin shows little or no centrality dependence. The EPS09s nPDF based calculations are consistent with the data at forward rapidity within uncertainties.

Quarkonia and open heavy-flavor hadrons are sensitive to the same effects on heavy-quark production. However, quarkonium states are additionally influenced by breakup in nuclear matter. Therefore, open heavy-flavor production can provide a baseline for interpreting the nuclear breakup of quarkonia. Previous measurements suggest that nuclear breakup has a significant effect on quarkonia production in nuclear collisions [21, 29–34].

Figure 4 shows a comparison of R_{dA} between heavy-flavor muons and J/ψ [21] for central collisions. A similar behavior across the entire p_T range is observed at forward rapidity, within the systematic uncertainties, whereas a distinct difference is seen at backward rapidity, particularly for $p_T < 2.5$ GeV/c where charm contributions dominate over those from bottom [35]. The larger difference of the R_{dA} between J/ψ and open charm at backward rapidity compared to forward rapidity could be related to the longer time this $c\bar{c}$ state requires to traverse the nuclear matter or the larger density of comoving particles after the initial collision at backward rapidity [36]. This comparison suggests that an additional CNM effect, nuclear breakup, significantly affects J/ψ production at mid- and backward rapidity. This measurement provides a key additional constraint on theoretical models attempting to describe quarkonia yields in nuclear collisions.

We have presented a measurement of negatively charged heavy-flavor muons produced at forward and backward rapidity in d+Au collisions at $\sqrt{s_{NN}} = 200$ GeV, for several centrality classes. We observe no significant modification in the most peripheral d+Au collisions. However, in central d+Au collisions, suppression (enhancement) of heavy-flavor muons is observed at forward (backward) rapidity. The large difference between forward and backward rapidity, which is not reproduced by PYTHIA calculations with the EPS09s nPDF sets, suggests that various CNM effects combine to produce the observed modifications. A comparison between the measured nuclear modification factors for J/ψ and open heavy-flavor production provides strong indication that nuclear breakup significantly affects quarkonia production.

We thank the staff of the Collider-Accelerator and Physics Departments at Brookhaven National Laboratory and the staff of the other PHENIX participating institutions for their vital contributions. We acknowledge support from the Office of Nuclear Physics in the Office of Science of the Department of Energy, the National Science Foundation, Abilene Christian University Research Council, Research Foundation of SUNY, and Dean of the College of Arts and Sciences, Vanderbilt University (U.S.A), Ministry of Education, Culture, Sports, Science, and Technology and the Japan Society for the Promotion of Science (Japan), Conselho Nacional de Desenvolvimento Científico e Tecnológico and Fundação de Amparo à Pesquisa do Estado de São Paulo (Brazil), Natural Science Foundation of China (P. R. China), Ministry of Education, Youth and Sports (Czech Republic), Centre National de la Recherche Scientifique, Commissariat à l'Énergie Atomique, and Institut National de Physique Nucléaire et de Physique des Particules (France), Bundesministerium für Bildung und Forschung, Deutscher Akademischer Austausch Dienst, and Alexander von Humboldt Stiftung (Germany), Hungarian National Science Fund, OTKA (Hungary), Department of Atomic Energy and Department of Science and Technology (India), Israel Science Foundation (Israel), National Research Foundation and WCU program of the Ministry Education Science and Technology (Korea), Physics Department, Lahore University of Management Sciences (Pakistan), Ministry of Education and Science, Russian Academy of Sciences, Federal Agency of Atomic Energy (Russia), VR and Wallenberg Foundation (Sweden), the U.S. Civilian Research and Development Foundation for the Independent States of the Former Soviet Union, the Hungarian American Enterprise Scholarship Fund, the US-Hungarian Fulbright Foundation for Educational Exchange, and the US-Israel Binational Science Foundation.

---

[*] Deceased

[†] PHENIX Co-Spokesperson: morrison@bnl.gov

[‡] PHENIX Co-Spokesperson: jamie.nagle@colorado.edu

[1] B. Abelev et al. (ALICE Collaboration), arXiv:1203.2160.

[2] B. Abelev et al. (ALICE Collaboration), arXiv:1305.2707.

[3] S. S. Adler et al. (PHENIX Collaboration), Phys. Rev. D **76**, 092002 (2007).

[4] A. Adare et al. (PHENIX Collaboration), Phys. Rev. Lett. **97**, 252002 (2006).

[5] H. Agakishiev et al. (STAR Collaboration), Phys. Rev. D **83**, 052006 (2011).

[6] S. S. Adler et al. (PHENIX Collaboration), Phys. Rev. Lett. **96**, 032301 (2006).

[7] A. Adare et al. (PHENIX Collaboration), Phys. Rev. Lett. **98**, 172301 (2007).

[8] A. Adare et al. (PHENIX Collaboration), Phys. Rev. C **86**, 024909 (2012).

[9] M. G. Mustafa, Phys. Rev. C **72**, 014905 (2005).

[10] G. D. Moore and D. Teaney, Phys. Rev. C **71**, 064904 (2005).

[11] H. van Hees, V. Greco, and R. Rapp, Phys. Rev. C **73**, 034913 (2006).

[12] M. Djordjevic, arXiv:nucl-th/0603066.

[13] K. J. Eskola, H. Paukkunen, and C. A. Salgado, JHEP **0904**, 065 (2009).

[14] I. Helenius, K. J. Eskola, H. Honkanen, and C. A. Salgado, JHEP **1207**, 073 (2012).

[15] T. Sjostrand, S. Mrenna, and P. Z. Skands, JHEP **0605**, 026 (2006), version 8.176 with hard processes *HardQCD:gg2ccbar* and *HardQCD:qqbar2ccbar* decaying to muons and all other parameters set to the default values. url=http://www.hepforge.org/lists-archive/pythia8-announce/2013/

[16] I. Vitev, Phys. Rev. C **75**, 064906 (2007).

[17] A. Adare et al. (PHENIX Collaboration), arXiv:1208.1293.

[18] M. Allen et al. (PHENIX Collaboration), Nucl. Instrum. Methods A **499**, 549 (2003).

[19] S. N. White, Amer. Inst. Phys. Conf. Proc. **792**, 527 (2005).

[20] M. L. Miller, K. Reygers, S. J. Sanders, and P. Steinberg, Ann. Rev. Nucl. Part. Sci. **57**, 205 (2007).

[21] A. Adare et al. (PHENIX Collaboration), Phys. Rev. C **87**, 034904 (2013).

[22] A. Adare et al. (PHENIX Collaboration), arXiv:1304.3410.

[23] K. Adcox et al. (PHENIX Collaboration), Nucl. Instrum. Methods A **499**, 469 (2003).

[24] H. Akikawa et al. (PHENIX Collaboration), Nucl. Instrum. Methods A **499**, 537 (2003).

[25] A. Adare et al. (PHENIX Collaboration), Phys. Rev. C **84**, 044905 (2011).

[26] J. K. Yoh, S. W. Herb, D. C. Hom, L. M. Lederman, J. C. Sens, et al., Phys. Rev. Lett. **41**, 684 (1978).

[27] R. Sharma, I. Vitev, and B.-W. Zhang, Phys. Rev. C **80**, 054902 (2009).

[28] B. Abelev et al. (ALICE Collaboration), Phys. Rev. Lett. **109**, 112301 (2012).

[29] J. L. Nagle, A. D. Frawley, L. A. Linden Levy, and M. G. Wysocki, Phys. Rev. C **84**, 044911 (2011).

[30] A. Adare et al. (PHENIX Collaboration), Phys. Rev. C **77**, 024912 (2008).

[31] A. Adare et al. (PHENIX Collaboration), arXiv:1305.5516.

[32] A. Adare et al. (PHENIX Collaboration), Phys. Rev. Lett. **107**, 142301 (2011).
[33] B. Z. Kopeliovich, I. K. Potashnikova, and I. Schmidt, Nucl. Phys. A **864**, 203 (2011).
[34] C. Lourenco, R. Vogt, and H. K. Woehri, JHEP **0902**, 014 (2009).
[35] A. Adare et al. (PHENIX Collaboration), Phys. Rev. Lett. **103**, 082002 (2009).
[36] R. Vogt, Phys. Rev. C **61**, 035203 (2000).